Nutr Cycl Agroecosyst
DOI 10.1007/s10705-006-9025-y

ORIGINAL PAPER

Nitrogen cycling in an irrigated wheat system in Sonora, Mexico: measurements and modeling

L. Christensen · W. J. Riley · I. Ortiz-Monasterio

Received: 14 February 2005 / Accepted: 26 April 2006

Abstract An improved version of an ecosystem nitrogen cycling model (NLOSS) is described, tested, and used to analyze nitrogen cycling in the Yaqui Valley, Sonora, Mexico. In addition to previously described modules in NLOSS that simulate soil water and solute fluxes, soil evaporation, soil energy balance, and denitrification, modules were added to estimate crop growth, soil carbon cycling, urea hydrolysis, and nitrification. We first tested the model against season-long measurements of soil NO_3^-, NO_2^-, and NH_4^+ aqueous concentrations; NO and N_2O soil effluxes; and crop biomass accumulation in three fertilizer treatments. We used NLOSS to test the sensitivity of wheat production, NO_3^- losses, and trace-gas emissions to fertilizer application rate. With the model, we compared the typical farmer's fertilization of 250 kg N ha^{-1} with five other fertilization scenarios, ranging from 110 to 220 kg N ha^{-1}. The typical farmer's practice produced higher wheat yield than the lower fertilization treatments. However, the increase in yield per increase in kg N applied decreased with increasing fertilizer addition as a result of higher leaching losses, higher residual N, and higher trace-gas emissions. In addition, with respect to the lowest fertilization treatment, the highest fertilization treatment resulted in an 11% decrease, a 10% increase, and a 157% increase in N_2, N_2O, and NO emissions, respectively, and a 41% increase in leached NO_3^- + NO_2^-. These results demonstrate that a small decrease in fertilizer application rate can increase N-use efficiency for wheat growth, while reducing leaching losses and emissions of harmful trace gas fluxes.

Keywords Crop growth · N_2 fluxes · N_2O fluxes · NO fluxes · NLOSS · Trace gas · Yaqui Valley

L. Christensen
Center for Environmental Science and Policy, Stanford University, Stanford, CA 94305, USA

W. J. Riley
Lawrence Berkeley National Laboratory, Berkeley, CA 94720, USA

I. Ortiz-Monasterio
CIMMYT, Mexico D.F. 06600, Mexico

Present address:
L. Christensen (✉)
Natural Resource Ecology Laboratory, Colorado State University, Ft. Collins, CO 80523, USA
e-mail: lindsey@nrel.colostate.edu

Introduction

The consequences of nitrogen (N) fertilizer use in agricultural ecosystems include some that are positive, such as increased crop yields and quality, and some that are negative, such as impacts to human

health and ecosystems. Adverse effects to human health include nitrate (NO_3^-) and nitrite (NO_2^-) drinking water contamination which can lead to methemoglobinemia (blue baby syndrome) (Elmi et al. 2002), respiratory and cardiac disease from exposure to high ozone (O_3) levels (of which nitric oxide (NO) is an important precursor) (US EPA 2003), and breathing difficulty and damage to lung tissue from particulate matter from nitrogen oxide precursors (US EPA 2003). Deleterious ecosystem impacts include soil acidification, eutrophication of freshwater systems, pollution of surface waters, increases in greenhouse gas concentrations, formation of tropospheric ozone, depletion of stratospheric O_3, and loss of biodiversity in coastal ecosystems (Matson et al. 1997; Fenn et al. 1998, 2003; Vitousek et al. 1998; Follett and Follett 2001).

Despite the knowledge on adverse effects, N application levels continue to increase and represent the largest anthropogenic N source to the environment (Vitousek and Matson 1993; Smil 1999). Agricultural fertilization has increased to support increased crop growth, resulting in a doubling, from pre-industrial times, of reactive N (i.e., ammonia (NH_3), ammonium (NH_4^+), NO, NO_2^-, nitrous oxide (N_2O), NO_3^-, and nitric acid (HNO_3)) production to 33 tera-grams N per year in 2000 (Galloway and Cowling 2002). Sources of nitrogenous atmospheric pollutants are expected to increase in the future, largely due to an increased need of fertilizer N for food production (Follett and Follett 2001; Galloway et al. 2002).

Approaches that analyze the complete N cycle in relation to crop growth (Galloway et al. 2002) allow more accurate assessment of N-use efficiency and losses of nitrogen to the atmosphere and water (Cassman et al. 2002). Sophisticated models have been developed that simulate N cycling and crop growth in agricultural ecosystems (e.g., CENTURY (Parton et al. 1996), DAYCENT (Parton et al. 1998), NLOSS (Riley and Matson 2000), and DNDC (Li et al. 1992), but uncertainties remain in simulating N losses (Smil 1999). For this study, the NLOSS model (Riley and Matson 2000; Riley et al. 2001) has been expanded to include nitrification, urea hydrolysis, plant growth, and carbon cycling submodels. These modules, with the existing denitrification and nitrate leaching submodels, allow us to examine N flows between ecosystem pools and between the ecosystem and atmosphere in a detailed and relatively mechanistic manner. In this paper we (1) test NLOSS against comprehensive season-long measurements of soil NO_3^-, NO_2^-, and NH_4^+ aqueous concentrations, NO and N_2O soil effluxes, and crop biomass accumulation in three fertilizer treatments and (2) use the model to examine the sensitivity of NO, N_2O, and N_2 gas fluxes, N leaching, and wheat biomass accumulation to fertilizer application rate.

Methods

Experimental site and model testing

We tested NLOSS using measurements from field experiments conducted in the Yaqui Valley near Ciudad Obregon, Sonora, Mexico (27° N109° W, 40 masl) (Panek et al. 2000). Details of soil characteristics, crop rotations, experimental area, and meteorological data are given in Riley and Matson (2000) and Riley et al. (2001). We briefly describe the site here. Wheat covers a large majority of the production land in winter (77% in 2003) and is therefore the focus of this study. Currently, the average N fertilizer application rate is about 250 kg N ha^{-1} per wheat crop cycle, with the most common practice being broadcast application of 66–75% of the total N as urea or injection of anhydrous ammonia before planting, followed by irrigation. The rest of the N fertilizer is applied around 45–55 days after plating as anhydrous ammonia.

The experimental area was planted with bread wheat (*Triticum aestivum* L. cultivar 'Rayon F89') following a soybean (*Glycine max* (L.) Merr) crop, in the 1995–1996 season. Following the 1995 summer crop harvest, the field was plowed, disked twice, and then leveled. The experimental area then received 20 kg P ha^{-1} as triple superphosphate, incorporated with the formation of 75 cm beds. The wheat was planted in two rows 20 cm apart on top of the bed at the rate of 100 kg seeds ha^{-1} (Panek et al. 2000).

Three experimental treatments (ET1, ET2, ET3) applied different doses of fertilizer at different application times: (ET1) 312.5 kg N ha^{-1} as

urea-N, with 60% applied three weeks prior to planting and 40% 5 weeks after planting; (ET2) 250 kg N ha^{-1} as urea-N, with 33% applied at planting and 67% 5 weeks after planting; and (ET3) 180 kg N ha^{-1} as urea-N, with 33% applied at planting and 67% 5 weeks after planting (Panek et al. 2000). A control treatment with no fertilizer addition (but with otherwise the same crop management) was also included. The experimental treatments were arranged in a randomized complete block design with four replications. The plots in all three treatments were furrow-irrigated following the method and schedule used by most farmers in the area (Table 1). Cultivation and thorough hand weeding were used to keep the experimental area weed free. In each treatment, the following measurements were made throughout the growing season: N_2O, NO, and N_2 surface fluxes (Panek et al. 2000); soil concentrations of NH_4^+, NO_3^-, and NO_2^- (Riley et al. 2001); soil moisture and temperature (Riley et al. 2001); and crop biomass. Nitrogen trace gas fluxes were measured using 25 cm diameter polyvinyl chloride rings. Plastic chambers were placed over the rings where N_2O, NO, and N_2 measurements (collected midday) were taken (Panek et al. 2000). Lysimeters were installed and monitored in the fields for NH_4^+, NO_3^-, and NO_2^- measurements (Riley et al. 2001). The measurements were made separately in beds and furrows, and given here as area-weighted averages. Above ground biomass was collected from an area of 0.5 m^2 and oven dried for 24 h at 75°C on specified days throughout the growing season in ET1 and ET2.

Input datasets

The meteorological driving variables necessary to run NLOSS include: above-canopy air temperature, shortwave solar radiation, wind speed, precipitation, relative humidity, and vapor pressure deficit. These parameters were obtained at 0.5 h intervals from a weather station 2 km from the experimental fields used in this study (http://www.ag.arizona.edu/azmet/azdata.htm). Initial soil nitrate content in the experimental treatments was based on site measurements (Panek et al. 2000).

Model description

The NLOSS model attempts to include, in a relatively mechanistic manner, the physical, chemical, and biological processes that impact N cycling in ecosystems and exchanges between the ecosystem and atmosphere. The methods used to simulate soil water and solute fluxes, soil evaporation, soil

Table 1 Irrigation, fertilization, and planting information for the three experimental treatments in the 1995–1996 growing season

Experimental treatment	Irrigation dates	Irrigation amount(m)	Fertilization dates	Fertilizer applied(kg N ha^{-1})	Planting date
ET1	11/6/1995	0.10	11/3/1995	187.5 Urea	11/23/1995
	1/3/1996	0.08	1/3/1996	125.0 NH_3	
	1/29/1996	0.08			
	2/29/1996	0.08			
	3/7/1996	0.08			
	3/22/1996	0.08			
ET2	11/6/1995	0.10	11/23/1995	82.5 Urea	11/23/1995
	1/2/1996	0.08	1/2/1996	167.5 Urea	
	1/29/1996	0.08			
	2/29/1996	0.08			
	3/7/1996	0.08			
	3/22/1996	0.08			
ET3	11/10/1995	0.10	11/8/1995	59.4 Urea	12/1/1995
	1/4/1996	0.08	1/4/1996	120.6 Urea	
	1/26/1996	0.08			
	2/19/1996	0.08			
	3/4/1996	0.08			
	3/17/1996	0.08			

Irrigation amounts were the same for all three treatments, although irrigation application was not always on the same day

energy balance, and soil trace-gas generation, transport, and exchange with soil water are described in Riley and Matson (2000). We briefly describe these submodels, and then the new submodels that have been added to simulate crop growth, soil carbon cycling, urea hydrolysis, nitrification, and NH_3 losses. NLOSS accurately predicted denitrified N_2 and disaggregated nitrified and denitrified N_2O surface fluxes over a two-week period (Riley and Matson 2000). The model has also been applied, in the same region, to study the impact on N leaching of several N fertilizer application and irrigation strategies (Riley et al. 2001).

NLOSS applies the Richards equation with a 10 cm vertical discretization to compute soil moisture and water fluxes. A no-flux boundary condition is imposed at the bottom of the column (1 m). The FAO Penman-Monteith approach (Allen et al. 1994) is used to estimate latent heat fluxes. Soil temperature is calculated with a Fourier conduction model using soil-moisture dependent estimates of bulk soil heat capacity. The denitrification submodel applies Michaelis–Menten kinetics to simulate N transfers between NO_3^-, NO_2^-, N_2O, and N_2. Denitrification occurs only in the anaerobic fraction of soil, which is estimated using the method of Arah and Vinten (1995). The gas diffusion coefficient depends on temperature and soil moisture, and is estimated using the approach of Moldrup et al. (1999).

The remainder of this subsection describes the new submodels that have been added to the NLOSS model.

Nitrification submodel

NLOSS's nitrification submodel predicts the rate and byproducts of microbial nitrification ($NH_4^+ \rightarrow NO_3^-$). We model the nitrification rate, R_N (kg N m^{-2} s^{-1}) in the top soil layer only, as (Firestone and Davidson 1989):

$$R_N = ATMC_N \quad (1)$$

where A is an empirical constant, T is a temperature factor, M is a moisture factor, and C_N is the soil solution NH_4^+ concentration. This method is similar to methods used in CENTURY (Parton et al. 1996) and DNDC (Li et al. 1992). A moisture- and temperature-dependent factor, f_1, is used to compute the fraction of the nitrification rate emitted as a gas, and a moisture-dependent factor, f_2, is applied to separate the nitrified NO and N_2O gas emissions:

$$F_{NO} = f_1 f_2 R_N \quad (2)$$

$$F_{N_2O} = f_1(1 - f_2)R_N \quad (3)$$

where F_{NO} and F_{N_2O} are the nitrification NO and N_2O effluxes (kg N m^{-2} s^{-1}), respectively. We developed the relationships for f_1 and f_2 using a study that applied ^{15}N as a tracer to partition measured N_2O fluxes into nitrified and denitrified N_2O fluxes (Panek et al. 2000).

Carbon cycling submodel

NLOSS's prediction of soil carbon cycling is based on the decomposition model used in DNDC (Li et al. 1992). In this approach, soil carbon is divided into three organic matter pools: residues, microbial biomass, and humads. Each of the three pools is further divided into labile and resistant fractions. Decomposition is modeled as pseudo-first order decay from each of these pools with rate constants that are a function of the pool's potential decomposition rate, soil temperature, and soil moisture. A soluble C pool (used in the denitrification and aqueous transport calculations) with mass based on the rate of microbial biomass and humads decomposition is also simulated. Soil N cycling is tied to carbon transformations, since each C transfer between pools requires a concurrent transfer of N. C flow limitations will occur when there is insufficient N to complete the transfer (we assume fixed C/N ratios of the pools, as described in Riley and Matson (2000)). Conversely, surplus N from a C flow is returned to the soil mineral N pool.

Crop growth submodel

Crops play an important role in C and N cycling in managed ecosystems. We have included in NLOSS the CERES crop growth submodel (Ritchie 1991) for the wheat planted in the experimental treatments. This submodel computes crop biomass and grain accumulation at a

daily time step, N demand and accumulation, and other intermediate parameters (e.g., LAI) important in the prediction of plant dynamics. The crop growth submodel is called daily and takes as input daily total solar radiation, daily minimum and maximum air temperatures, daily-averaged soil N and C levels (as calculated in the carbon and nitrogen cycling submodels), and daily-averaged soil moisture.

Urea hydrolysis

In the Yaqui Valley, farmers apply urea as granules broadcast on the beds, or incorporated during bed formation. The rate at which urea hydrolyzes to NH_4^+ depends on soil pH, organic carbon content, moisture, and temperature. There is substantial uncertainty in determining the urea hydrolysis rate. For the results shown here, we applied the CERES approach (Ritchie 1991).

Ammonia loss during fertilization

There are no published studies quantifying ammonia losses following fertilization in the Yaqui Valley, although conditions are favorable due to high soil pH levels (Panek et al. 2000) and N application rates. Although not quantifiable, relative losses from ammonia fluxes, measured using acid traps, were very high relative to other agricultural systems (unpublished data). We used the method of Ismail et al. (1991) to estimate the fraction of added N lost as NH_3. Ammonia volatilization, by this method, is a function of soil temperature, soil pH, soil moisture content, urea application rate, and urea application depth.

Monte Carlo simulations

We applied a Monte Carlo method to quantify uncertainty in model predictions resulting from uncertainty in submodel parameterizations. Log-normal distributions were assumed for parameters in the soil moisture, denitrification, and nitrification submodels, and for fertilizer and irrigation inputs. Two hundred simulations were conducted for each Monte Carlo run, and mean and uncertainty ranges (taken as 1 standard deviation (SD) of the ensemble predictions) were computed for the model predictions of interest (e.g., NO_3^- levels). Note that in the figures we present this 1 SD range as 'error bars' about the mean prediction. A geometric standard deviation (GSD) of 1.2 is used for all parameters that vary in the Monte Carlo simulations (Riley and Matson 2000). Geometric means for parameters in the hydrologic, denitrification, and anaerobic fraction models are the same as those shown in Tables 1 and 2 of Riley and Matson (2000). We also apply the GSD of 1.2 to the parameters used to simulate urea hydrolysis and nitrification.

Model application

Following model testing, NLOSS was used to simulate six fertilizer treatments (ST1, ST2, ST3, ST4, ST5, and ST6) in the Yaqui Valley. Meteorological and irrigation inputs for the six treatments were the same as those used to test the model. Fertilizer doses (Table 2) encompass a range from the high levels currently being applied to low levels suggested by the Mexican Secretaría de Agricultura (SAGARPA 2001). Model predictions of crop biomass; cumulative NO, N_2O, and N_2 gas emissions; cumulative NO_3^- + NO_2^-

Table 2 Parameters used in NLOSS for the six simulated fertilization treatments

For all six simulated treatments, the first and second fertilizer applications are 75 and 25% of the total, respectively

Experimental treatment	Application 1 (kg N ha^{-1}) day 3	Application 2 (kg N ha^{-1}) day 64	Totals (kg N ha^{-1})
ST1	86.25	28.75	115.00
ST2	97.50	32.50	130.00
ST3	120.00	40.00	160.00
ST4	142.50	47.50	190.00
ST5	165.00	55.00	220.00
ST6	187.50	62.50	250.00

leaching; and residual soil NH_4^+ levels for the various treatments were compared.

Results and discussion

Model testing

NLOSS simulated water-filled pore space (WFPS) accurately in the 0–15 cm range during the simulation period (Fig. 1). Predicted WFPS at the two deeper depth increments (15–30 cm and 30–60 cm) differed from measurements by less than 10% WFPS across the season, and were most accurate in the latter part of the season (after March '96).

NLOSS accurately simulated trends in NH_4^+ levels in the three experimental treatments, including onset, peaks, and decreases over the season (Fig. 2). Peaks in NH_4^+ concentration coincided with fertilizer application; concentration changes over time were impacted by urea hydrolysis, ammonia volatilization, plant uptake, microbial immobilization and release, and nitrification to NO_3^-. NLOSS underestimated NH_4^+ concentrations in ET1, and overestimated NH_4^+ concentrations in ET2.

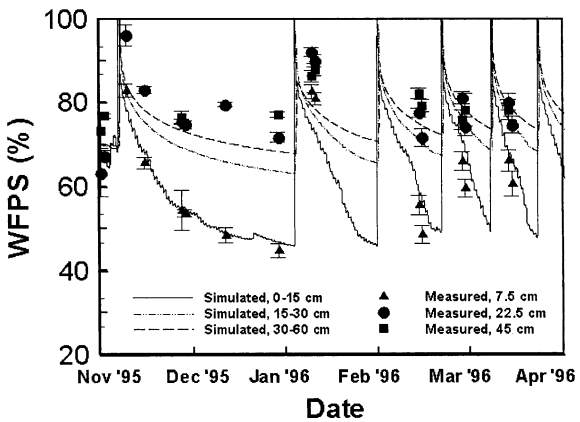

Fig. 1 Measured and simulated water-filled pore space (WFPS) at three soil depths over the 1995–1996 wheat season. Model estimates were most accurate in the top 15 cm, while simulated trends were accurate in all three layers. Error bars represent ±1 SE of four replicate plots

NLOSS estimates the N leaching flux as the product of aqueous $NO_3^- + NO_2^-$ concentrations at 70–80 cm depth and the simulated water flux (Riley et al. 2001). As described in that paper, predicted leached N fluxes in ET1 were substantially higher than in ET2 and ET3, as a result of the substantially larger fertilizer N applied in ET1. NLOSS nitrification and denitrification submodels accurately predicted N_2O and NO emissions (Fig. 3). Onset and seasonal trends of N_2O production closely followed observations, however, model simulations predicted high, short-lived N_2O pulses immediately following irrigation events that were not always observed in the measurements. This observation does not necessarily imply inaccuracy in model predictions, but may be due to high variability in N_2O production, particularly immediately following irrigation, that is difficult to capture in periodic soil flux chamber measurements. In either case, the integrated N_2O efflux associated with these peaks is a small fraction of the predicted cumulative flux to the atmosphere. NLOSS accurately predicted NO emissions, with onset and decreases in NO production closely following measurements.

NLOSS simulated the trend in plant production accurately for both ET1 and ET2 (Fig. 4). In

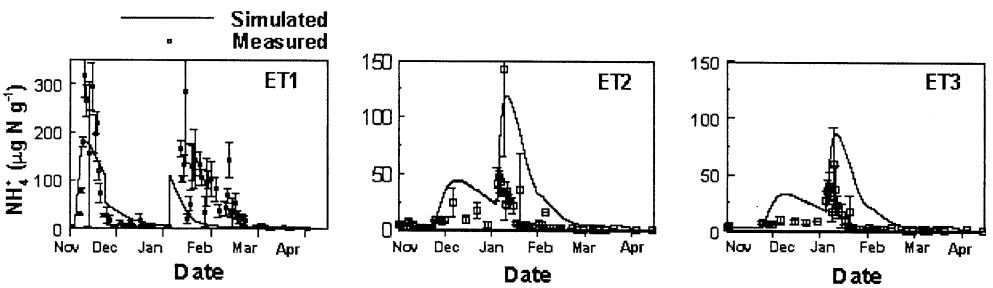

Fig. 2 Measured and simulated aqueous NH_4^+ concentrations for three experimental treatments (ET1, ET2, and ET3) over the 1995–1996 growing season. Error bars represent ±1 SE of four replicate plots

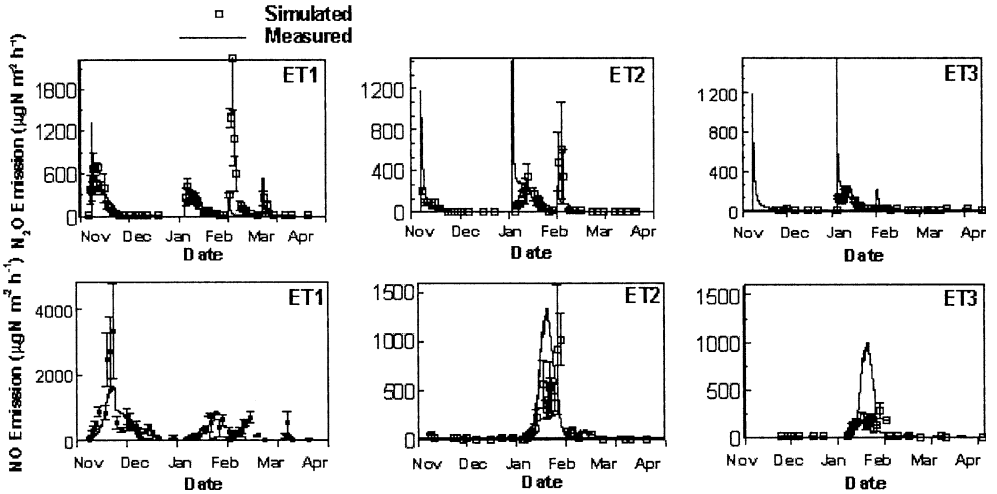

Fig. 3 Measurements and simulations of N_2O and NO surface fluxes for three experimental treatments (ET1, ET2, and ET3) over the 1995–1996 growing season. Model simulations accurately predicted onset and trend in N_2O and NO production. Peak NO fluxes were underestimated for ET1 and overestimated for ET3. Error bars represent ±1 SE of four replicate plots

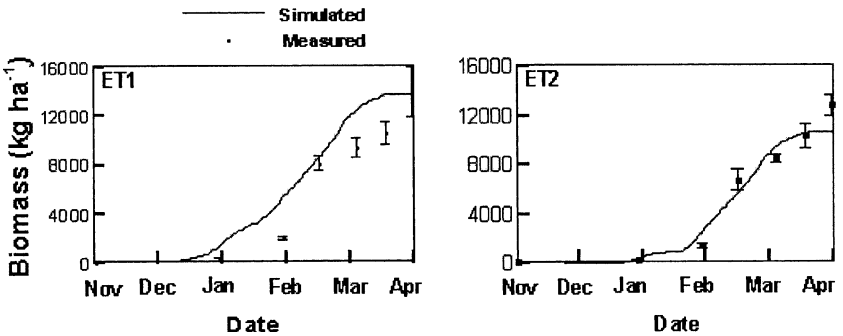

Fig. 4 Measurements and simulations of biomass production over the 1995–1996 growing season in experimental treatments 1 (ET1) and 2 (ET2). Model estimates accurately predicted trends and cumulative crop biomass

ET1, biomass values at the end of the season matched measured values, whereas in ET2, the trend in crop growth was more accurate but final biomass was 17% lower than measured values.

Model simulated treatments

For the simulated treatments (ST1–ST6), NLOSS predicted column-integrated (to 1 m) residual NH_4^+ at the end of the season that varied from 35 kg N ha^{-1} to 60 kg N ha^{-1} (Fig. 5). The increase in residual NH_4^+ per unit increase in N applied was fairly constant across all treatments. Cumulative N leaching over the crop cycle increased approximately 41% from the low to the high fertilizer application rate scenarios (Fig. 6); note that the N leached was still a small fraction of total N applied.

The NLOSS simulations showed a slight increase in total residual soil NO_2^- with increasing fertilizer application (Fig. 7). NO_2^- kinetics are rapid; in all treatments residual NO_2^- concentrations between treatments were relatively low compared to NO_3^- concentrations. Cumulative NO (Fig. 8) and N_2O (Fig. 9) fluxes increased substantially and only slightly, respectively, with increasing fertilizer application.

The relatively small increase in predicted cumulative N_2O production as compared to NO production was unexpected. To identify the mechanisms in the model influencing this response, we re-examined three treatments in more detail: 250 (ST1), 200 (ST3), and 150 (ST6) kg N ha^{-1}. Denitrified N_2O efflux after the first fertilization and irrigation was about the same between treatments (not shown). During sub-

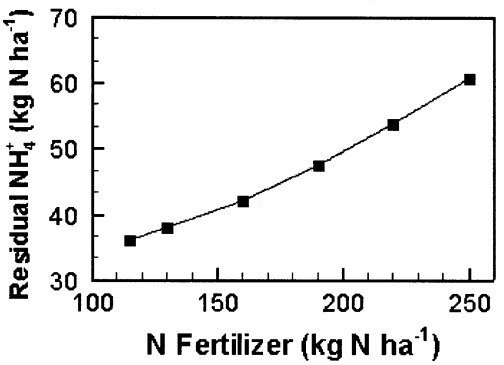

Fig. 5 Residual NH_4^+ integrated to 1 m depth at end of season for the six simulated treatments. There is an approximately linear increase in residual NH_4^+ with increasing fertilizer application

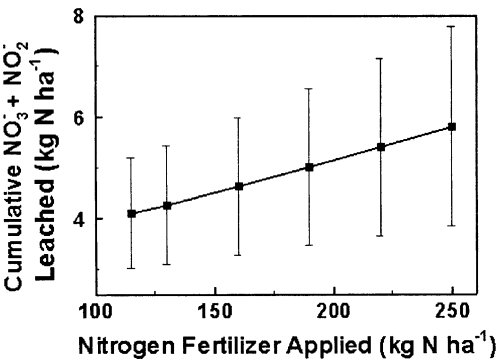

Fig. 6 Cumulative NO_3^- + NO_2^- leached over the season for the six simulated treatments. There is a slight increase in N leachate with increasing fertilizer application. Error bars indicate 1 SD of the Monte Carlo simulation predictions

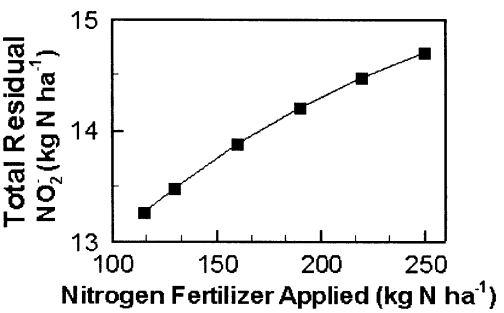

Fig. 7 Residual column-integrated NO_2^- concentrations for the six simulated treatments. NO_2^- concentrations increased slightly with increasing fertilizer application

sequent fertilization and irrigation events, the denitrified N_2O flux decreased with increasing fertilizer application (Fig. 10a shows the period

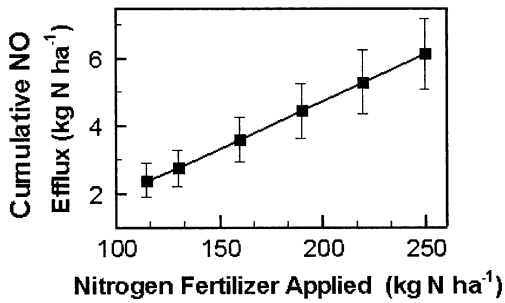

Fig. 8 Cumulative NO surface fluxes to the atmosphere for the six simulated treatments. Cumulative NO surface flux increased by 157% over the range of fertilizer application rates. Error bars indicate 1 SD of the Monte Carlo simulation predictions

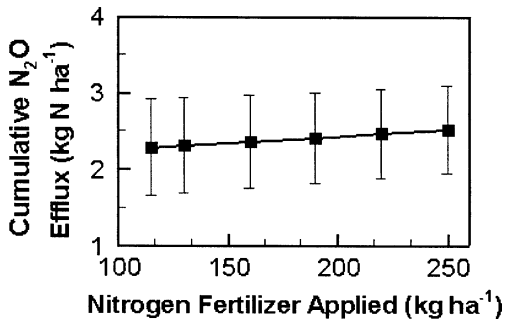

Fig. 9 Cumulative N_2O surface fluxes to the atmosphere from nitrification and denitrification for the six simulated treatments. Only a slight increase in cumulative N_2O efflux occurred as compared to the NO surface flux. Error bars indicate 1 SD of the Monte Carlo simulation predictions

surrounding the second fertilization and irrigation event).

At higher fertilizer doses, residual NO_3^- in the soil at the time of the subsequent fertilization is also higher (Fig. 10b). While in magnitude the differences in NO_3^- levels are small, these differences can impact the relative transformation rates in the modeled denitrification N cycle. Residual NO_2^- at the beginning of the irrigation was not substantially different among fertilizer rate treatments due to the rapid transformation to NO_3^-. As irrigation water is applied (JD 63), denitrification begins. The trace-gas surface fluxes begin after the soil moisture has reduced sufficiently to allow soil-gas diffusion within the column.

Figure 10(c) showed predicted N transformation rates (in the first soil layer) between NO_3^- and NO_2^-, R_1 (kg N m^{-3} s^{-1}), and between NO_2^- and

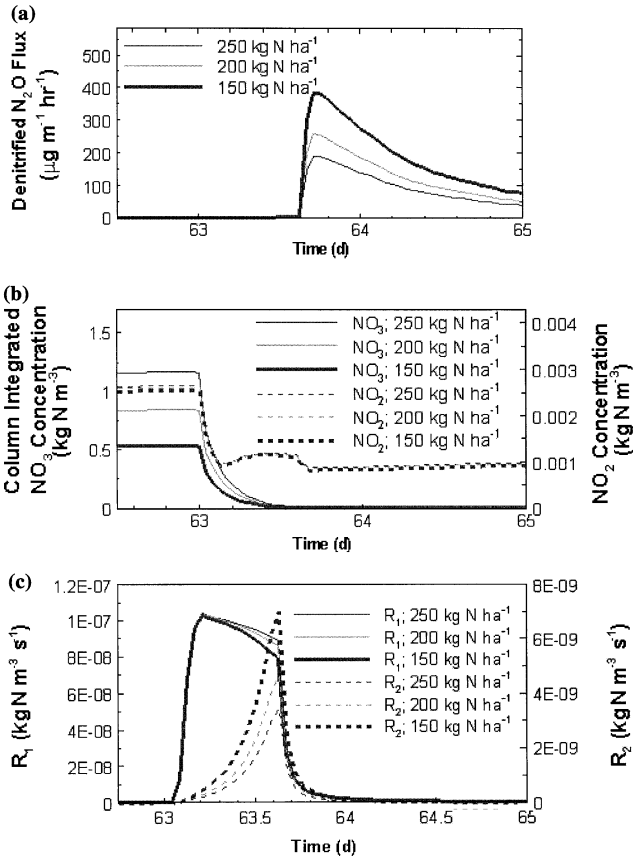

Fig. 10 (**a**) Predicted N_2O efflux immediately before and after the second irrigation for simulated treatments ST1, ST3, and ST6. (**b**) NO_3^- (solid lines) and NO_2^- (dotted lines) aqueous concentrations for the three simulated treatments. (**c**) N transformation rates between NO_3^- and NO_2^- (R1) (solid lines), and between NO_2^- and N_2O (R2) (dotted lines) for the three simulated treatments. These figures demonstrate why NLOSS predicts only slight increases in cumulative N_2O and N_2 emissions

N_2O, R_2 (kg N m^{-3} s^{-1}). Note that R_1 was largest with the largest N application rate, and R_2 was largest with the smallest N application rate. Therefore, with increased NO_3^- concentrations from increased fertilizer application, the relative transformation rate between NO_3^- and NO_2^- was higher than the relative transformation rate between NO_2^- and N_2O, thereby reducing the N_2O surface flux. Although consistent with our current understanding of N transformations during denitrification, further work is required to determine the extent to which these dynamics occur in real soils.

Mean Monte Carlo predicted cumulative N_2 emissions decreased slightly with increasing fertilizer application (Fig. 11). N_2 production occurs after N_2O production in the denitrification chain, so analogous arguments to those posed above explain this lower production.

NLOSS estimates of biomass accumulation increased with increasing N fertilizer application rate (Fig. 12). However, biomass accumulated per kg fertilizer applied (Nitrogen Use Efficiency, NUE) decreased with higher N fertilization rates (Figure 13). This decrease is the result of: (1) increased trace-gas losses (Figs. 9, 10); (2) increased leaching losses (Fig. 6); and (3) higher residual N at the end of the season. From this information we conclude that wheat production is maximized at fertilization application rates substantially below those used in standard practice in the Yaqui Valley. Because farmers do not have a reliable way of assessing residual N, they continue to apply high levels of fertilizer to guarantee suf-

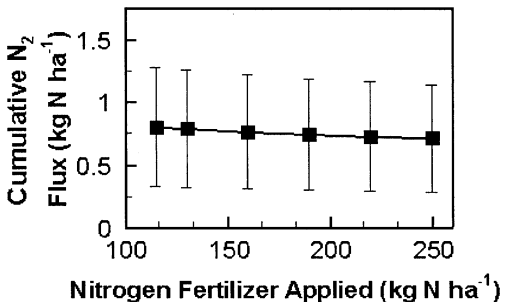

Fig. 11 Cumulative denitrified N_2 surface flux for the six simulated treatments. Model estimates show a slight decrease in N_2 production with increasing fertilizer application. Error bars indicate 1 SD of the Monte Carlo simulation predictions

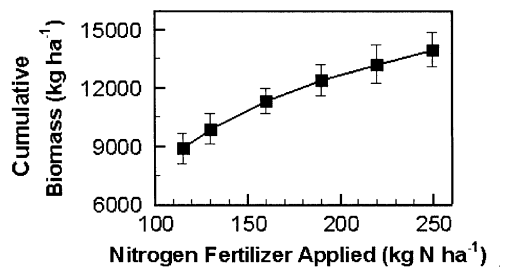

Fig. 12 Cumulative biomass at the end of season for the six simulated treatments. While biomass increases over the six simulated treatments, the rate of increase with increasing fertilizer application rates declines at the higher fertilization levels. Error bars indicate 1 SD of the Monte Carlo simulation predictions

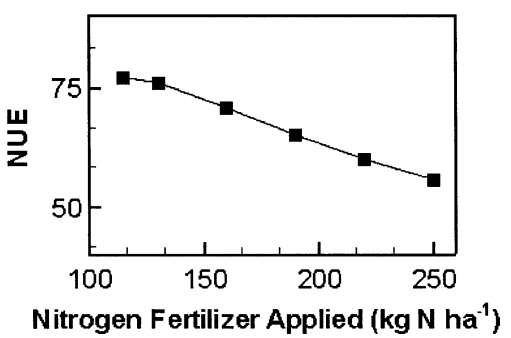

Fig. 13 Nitrogen Use Efficiency (NUE) as affected by fertilizer application on six simulated treatments

ficient soil N (Lobell et al. 2004). Further, the high levels of fertilizer application led to an 11% decrease, a 10% increase, and a 157% increase in N_2, N_2O, and NO cumulative gas effluxes, respectively, and a 41% increase in cumulative NO_3^- and NO_2^- leaching.

Conclusions

We applied NLOSS to examine N flows between ecosystem pools and between the ecosystem and the atmosphere in the Yaqui Valley, Mexico. NLOSS includes submodels of soil water and solute transport, urea hydrolysis, ammonification, nitrification, denitrification, nitrate leaching, and plant growth. We used the model to quantify the impact of fertilizer application rate on wheat production, nitrate losses, and nitrogen trace-gas emissions.

Simulations of WFPS were most accurate in the upper soil layers; predictions in the two deeper layers were consistently accurate to within ~10% WFPS. We compared NLOSS predictions to measurements in three experimental treatments. NLOSS accurately predicted trends in soil water NH_4^+, NO_3^-, and NO_2^- concentrations. Simulated N_2O and NO emissions closely followed measurements, except for predicted spikes immediately after irrigation. These discrepancies may reflect problems with the model or may be a result of intermittent data collection. NLOSS simulations of wheat biomass accumulation also closely matched measurements, as did the relative impact of different fertilizer application rates.

The model sensitivity analysis using six fertilizer treatments demonstrated the typical farmer's practice of applying 250 kg N ha^{-1} produced wheat biomass 57% higher than the lowest fertilizer treatment. However, the increase in total biomass per kg N fertilizer applied decreased with increasing application rates. In addition, NLOSS predicted an 11% decrease, a 10% increase, and a 157% increase in N_2, N_2O, and NO cumulative gas effluxes, respectively, and a 41% increase in cumulative leached $NO_3^- + NO_2^-$.

Nitrogen fertilization rates are very high in the Yaqui Valley, and therefore negative environmental impacts of farming are likely to be substantial. Results from NLOSS simulations show a small decrease in fertilizer application rate can result in higher agronomic N-use efficiency for wheat, while reducing harmful trace gas emissions and leaching under the simulated climate and irrigation management. There are other aspects of management that are important

to crop production, such as timing of fertilizer application, residual soil N levels, etc., that can be addressed. For example, in this study, peaks in N_2O and $NO_3^- + NO_2^-$ losses occurred at each irrigation event, at rates depending on fertilizer rate. Also, farmers need to know residual soil N levels in order to quantify reductions in fertilizer applications. A study by Lobell et al. (2004) shows the ability to estimate residual N can reduce N fertilization rates by 35%. Understanding the complicated interactions between fertilizer application methods (i.e., rate, form, and timing) and biological, chemical, and physical controls on ecosystem N cycling can help managers improve N-use efficiency in this region, and thereby improve crop production and return on investment while minimizing environmental impacts and potential human health hazards.

Acknowledgments This article is based on research supported in part by a grant from the National Science Foundation (award BCS-0004236) with contributions from the National Oceanic and Atmospheric Administration's Office of Global Programs for the Sustainability Systems Project. We would like to thank the anonymous reviewers for their suggestions and comments.

References

Allen RG, Smith M, Perrier A, Pereira S (1994) An update for the definition of reference evapotranspiration. ICID Bull 43:1–92

Arah JRM, Vinten AJA (1995) Simplified models of anoxia and denitrification in aggregated and simple-structured soils. Eur J Soil Sci 46:507–517

Cassman KG, Dobermann A, Walters DT (2002) Agroecosystems, nitrogen-use efficiency, and nitrogen management. Ambio 31:132–140

Elmi AA, Madramootoo C, Egeh M, Liu A, Hamel C (2002) Environmental and agronomic implications of water table and nitrogen fertilization management. J Environ Qual 31:1858–1867

Fenn ME, Poth MA, Aber JD, Baron JS, Bormann BT, Johnson DW, Lemly AD, McNulty SG, Ryan DR, Stottlemyer R (1998) Nitrogen excess in North American ecosystems: predisposing factors, ecosystem responses, and management strategies. Ecol Appl 8:706–733

Fenn ME, Baron JS, Allen EB, Rueth HM, Nydick KR, Geiser L, Bowman WD, Sickman JO, Meixner T, Johnsonk DW, Neitlich P (2003) Ecological effects of nitrogen deposition in the Western United States. BioScience 53:404–420

Firestone MK, Davidson EA (1989) Microbial basis of NO and N_2O production and consumption in soils. In: Andrai MO, Schimel DS (eds) Exchange of trace gases between terrestrial ecosystems and the atmosphere. John Wiley, New York, pp 7–21

Follett JR, Follett RF (2001) Utilization and metabolism of nitrogen by humans. In: Follett RF, Hatfield JL (eds) Nitrogen in the environment: sources, problems, and management. Elsevier, Amsterdam, pp 65–92

Galloway JN, Cowling EB (2002) Reactive nitrogen and the world: 200 years of Change. Ambio 31:64–71

Galloway JN, Cowling EB, Seitzinger SP, Socolow RH (2002) Reactive nitrogen: too much of a good thing. Ambio 31:60–63

Ismail KM, Wheaton FW, Douglas LW, Potts W (1991) Modeling ammonia volatilization from loamy sand soil treated with liquid urea. Trans ASAE 34:756–763

Li C, Frolking S, Frolking T (1992) A model of nitrous oxide evolution from soil driven by rainfall events: 1. Model structure and sensitivity. J Geophys Res 97:9757–9776

Lobell DB, Ortiz-Monasterio JI, Asner GP (2004) Relative importance of soil and climate variability for nitrogen management in irrigated wheat. Field Crops Res 87:155–165

Matson PA, Parton WJ, Power AG, Swift MJ (1997) Agricultural intensification and ecosystem properties. Science 277:504–509

Moldrup P, Olesen T, Yamaguchi T, Schjonning P, Rolston DE (1999) Modeling diffusion and reaction in soils: IX. The Buckingham–Burdine–Campbell equation for gas diffusivity in undisturbed soil. Soil Sci 164:542–551

Panek JA, Matson PA, Ortiz-Monasterio I, Brooks P (2000) Distinguishing nitrification and denitrification sources of N_2O in a Mexican wheat system using N-15. Ecol Appl 10:506–514

Parton WJ, Mosier AR, Ojima DS, Valentine DW, Schimel DS, Weier K, Kulmala AE (1996) Generalized model for N_2 and N_2O production from nitrification and denitrification. Global Biogeochem Cycles 10:401–413

Parton WJ, Hartman M, Ojima DS, Schimel DS (1998) DAYCENT: its land surface submodel: description and testing. Global Plant Change 19:35–48

Riley WJ, Matson PA (2000) NLOSS: a mechanistic model of denitrified N_2O and N_2 evolution from soil. Soil Sci 165:237–249

Riley WJ, Ortiz-Monasterio I, Matson PA (2001) Nitrogen leaching and soil nitrate, nitrite, and ammonium levels under irrigated wheat in Northern Mexico. Nutrient Cycling in Agroecosystems 61:223–236

Ritchie JT (1991) Wheat phasic development. In: Hanks J, Ritchie JR (eds) Modeling plant and soil systems. American Society of Agronomy, Madison WI, pp 31–54

SAGARPA (Secretaría de Agricultura, Ganadería, Desarrollo Rural, Pesca Y Alimentación). (2001). Guía Técnica Para Los Cultivos del Área de Influencia del Campo Experimental. Impreso y hecho en Mexico. Obregón, Sonora, México

Smil V (1999) Nitrogen in crop production: an account of global flows. Global Biogeochem Cycles 13:647–662

US EPA (Environmental Protection Agency) (2003) Latest findings on national air quality 2002 status and trends. Office of Air Quality Planning and Standards Emissions, Monitoring, and Analysis Division. Research Triangle Park, North Carollina

Vitousek PM, Matson PA (1993) Agriculture, the global nitrogen cycle, and trace gas flux. In: Oremland R (eds) Biogeochemistry of global change: radioactively active trace gases. Chapman and Hall, NY, pp 193–208

Vitousek PM, Hedin LO, Matson PA, Fownes JH, Neff J (1998) Within-system element cycles, input-output budgets, and nutrient limitation. In: Pace M, Groffman P (eds) Successes, limitations, and the future of ecosystem ecology. Springer, New York, pp 432–451